Photoluminescence characterization of quantum dot laser epitaxy

Y. Li *, Y. C. Xin, H. Su and L. F. Lester
Center for High Technology Materials, University of New Mexico
1313 Goddard SE, Albuquerque, NM 87106
A. L. Gray, S. Luong, K. Sun, Z. Zou, and J. Zilko
Zia Laser, Inc., Albuquerque, NM 87106

ABSTRACT

The correlations between the photoluminescence (PL) wavelength, integrated intensity, peak intensity, and FWHM with laser diode performance such as the maximum gain, injection efficiency, and transparency current density are studied in this work. The primary outcome is that the variation in PL intensity within a wafer originates primarily from differences in the radiative and non-radiative recombination rates and not from dot density variation. PL generated from 980 nm wavelength pumping appears to give more consistent data in assessing the optical quality of quantum dots that emit in the 1300 nm from the ground state.

1. INTRODUCTION

Quantum dot (QD) materials have been studied extensively in recent years [1-6]. Due to their delta-like density of states of QDs, lasers fabricated from these novel materials provide many superior characteristics such as ultralow threshold current [2,3], low temperature dependence of the threshold current [4], low linewidth enhancement factor [5]. One shortcoming of the QD technology, though, is the small modal gain of optical active regions formed from dots. In reaction to this challenge, much effort has been expended to improve the maximum optical gain of InAs QD semiconductor lasers on GaAs substrates. Either increasing the dot density or adding more layer of dots have been attempted. In some cases, it appears that the optical gain does not always scale with an overall increase in dot density per layer. The reasons for this behavior are unclear at this time, but materials characterization data is a logical starting point to gain insight. However, the materials characterization of quantum dot layers is still in its infancy. The purpose of this work is to explore correlations between photoluminescence (PL) wavelength, integrated intensity, peak intensity, and FWHM with laser diode performance such as maximum gain, injection efficiency, and transparency current density.

As expected, it is observed that the PL peak intensity scales with QD layer number for values between 1 and 6. In this instance, one expects a direct correlation between the maximum available gain and the PL strength. However, within a wafer it is not clear what PL peak intensity variation indicates. The challenge is to separate the influence on the PL strength from dot density variation, non-radiative dots (dark dots), and changing recombination processes across the wafer. For one of the wafers under study, two areas where the PL intensity differs by as much as 8 times are identified. Lasers fabricated from these different regions and PL data indicate that the density of activated QDs are similar since the maximum gains, PL and lasing wavelengths, and PL FWHMís are nearly identical. However, the transparency current densities vary by a factor of 3. These results indicate that the source of the PL variation on this wafer originates from differing recombination rates and not dark dots or dot density changes.

2. PL MAPPING DATA AND WAFER DESCRIPTION

Generally speaking, the PL intensity and maximum gain in QD material increases when more layers of dots are added. Figure 1 shows the PL peak intensity as a function of QD layer number for 1, 3, and 6 stacks. One can see that the PL peak intensity almost linearly increases with quantum dot layer number, which also confirms that the optical pumping in uniform across the QD active layer.

* yanli@chtm.unm.edu; phone 1 505 272-7933; fax 1 505 272-7801

Quantum Dots, Nanoparticles, and Nanoclusters II, edited by Diana L. Huffaker, Pallab K. Bhattacharya, Proceedings of SPIE Vol. 5734 (SPIE, Bellingham, WA, 2005)
0277-786X/05/$15 · doi: 10.1117/12.597089

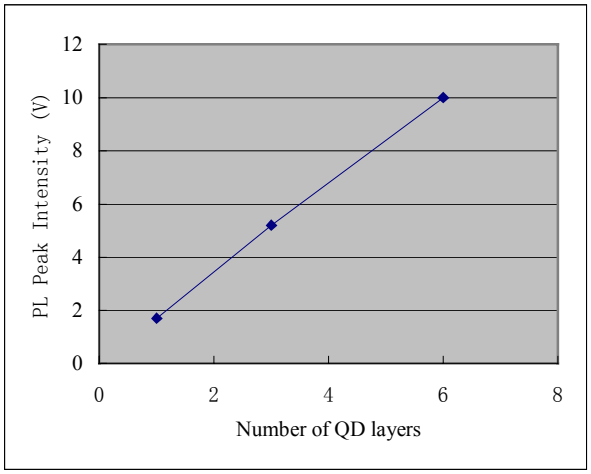

Figure 1. Relationship between PL peak intensity and the QD layer number.

However, in some cases, we have found that the PL intensity (or maximum modal gain) does not always scale with the dot density within a layer. The latter comparison is usually done from wafer to wafer. Here we present a study within a single QD laser wafer in which there is a huge difference in PL intensity in different sections of the slice. Figure 2 gives the layer structure of the wafer 207A. The quantum dots-in-a-well (DWELL) laser structure of 207A was grown by solid-source molecular beam epitaxy (MBE) on an n^+ GaAs substrate. The epitaxial layers consist of an n-type (10^{18} /cm^3) 300-nm-thick GaAs buffer, an n-type lower $Al_{0.7}Ga_{0.3}As$ cladding layer, a 315-nm-thick GaAs waveguide including the laser active region, a p-type upper cladding layer, and a p-doped (3×10^{19} cm^{-3}) 60-nm-thick GaAs cap. The cladding layers are doped at 10^{17} cm^{-3} and are each 2 μm thick. In the center of the waveguide, 6 DWELL layers with 29 nm GaAs barriers were grown. QDs with an equivalent coverage of approximately 2 monolayers of InAs are confined in the middle of a 10 nm thick $In_{0.15}Ga_{0.85}As$ QW in each layer. The QDs and QW were typically grown at 480-500 °C, as measured by an optical pyrometer. Each QD layer formed under these conditions has an areal density of about 1.3×10^{11} cm^{-2}, a base diameter <40nm, and are 7 nm high. Detailed descriptions of the DWELL growth technique can be found elsewhere.[2, 3, 6]

GaAs	p 3^{19}	60nm	
$Al_{.7->0}GaAs$	p 2^{19}	18nm	
$Al_{.7}Ga_{.3}As$	p 1^{17}	2000nm	
GaAs		26nm	
GaAs		29nm	} 6X
InAs/ $In_{.15}Ga_{.85}As$		10nm	
GaAs		55nm	
$Al_{.7}Ga_{.3}As$,	n1^{17}	2000nm	
$Al_{0->.7}GaAs$	n6^{17}	18nm	
GaAs	n 1^{18}	300nm	
GaAs N+ 2" substrate			

Figure 2. Structure of the 6-stack DWELL laser

PL mapping of the peak wavelength, peak intensity, integrated intensity and PL FWHMM was performed with an Accent PL mapper, the wavelength of the pumping laser being 532 nm. The results are shown in figure 3 with a 5-mm exclusion zone around the edge of the 2-inch wafer.

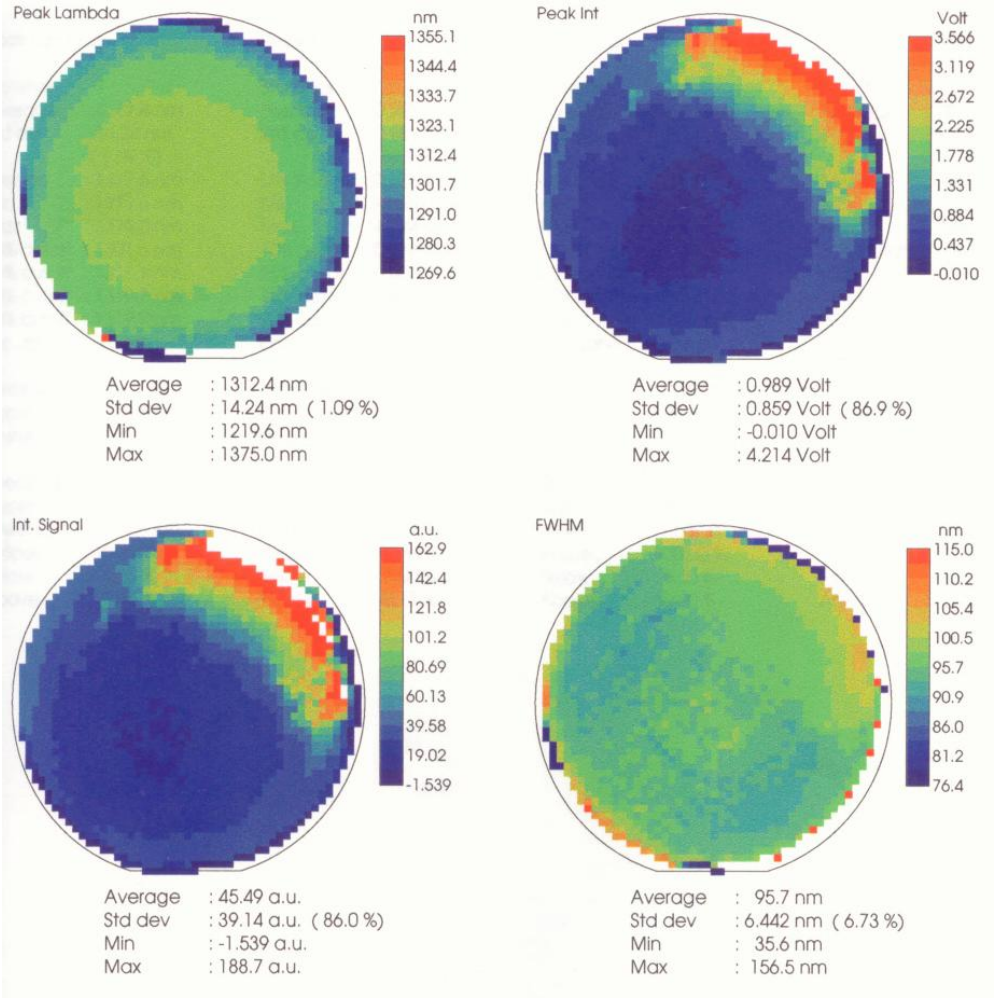

Figure 3. PL mapping data of sample 207A

From the maps above, it can be seen that the peak wavelength and FWHM are relatively uniform across the whole wafer with roughly radial symmetry. The standard deviations are only 1.09% and 6.73%, respectively. But there is a different outcome for the PL peak intensity and integrated intensity. The maximum values (in the "red" area in the upper-right corner) for the peak intensity and integrated intensity are eight times larger than the minimum values ("blue" area in the lower-left corner). So the key question is: Where does this huge difference come from? Does the "red" area have more quantum dots, a highly active dot density, or fewer defects in the dot layers than the "blue" area? Those questions canít be solved just relying on mapping data alone. We need to supplement the PL information with laser performance parameters. Normally, the maximum modal gain is proportional to dot density, so this a natural place to start.

3. LASER PERFORMANCE

For clarity, we introduce an identification scheme for pieces which the 2" wafer that is shown in figure 4. We picked two sample pieces "L" and "O" with the maximum PL intensity difference ("O" is the brighter) and fabricated into broad area lasers on them. Device fabrication begins with the formation of 50 μm wide stripes by Inductively Coupled Plasma

(ICP) etching followed by Ti/Pt/Au *p*-type contacts that are e-beam deposited. Finally, AuGe/Ni/Au *n*-type contacts are e-beam deposited after the substrate has been lapped down to a thickness of 125 μm.

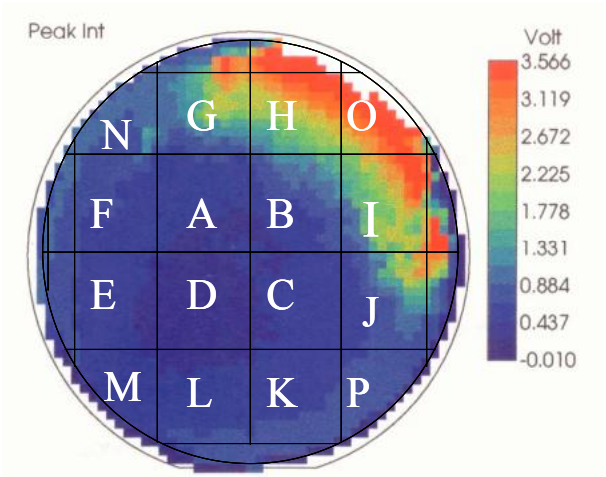

Figure 4. 2" wafer piece sections and location superimposed on the PL map

In figure 5, we give a comparison of the laser performance data including the maximum gain (g_{max}), transparency current (I_{tr}), injection efficiency (η_i), lasing wavelength and FWHM between the two samples. The maximum gain and transparency current were obtained by curve fitting the data for threshold gain (cavity loss) as a function of current for different cavity lengths. The two lasers have similar injection efficiency (33%), lasing wavelength (1275 nm), FWHM (96 nm) and maximum gain (19/cm), but the transparency current differs by as much as 3 times (254 mA in the "L" piece and 80 mA in the "O" piece). This indicates that the dot density or at least the active dot density is comparable between the two pieces. The difference in transparency current may result from defect related non-radiative recombination mechanisms such as Shockley-Read-Hall recombination.

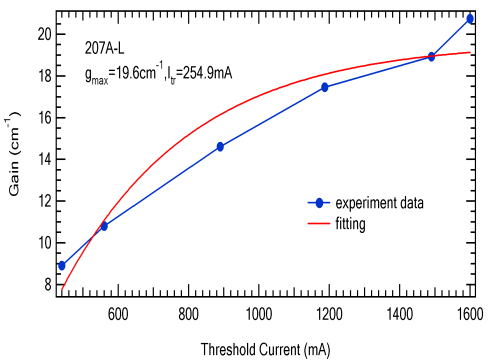

5(a)

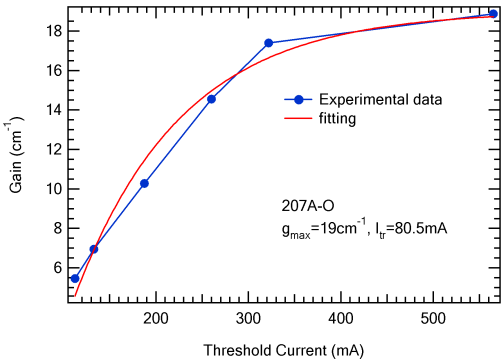

5(b)

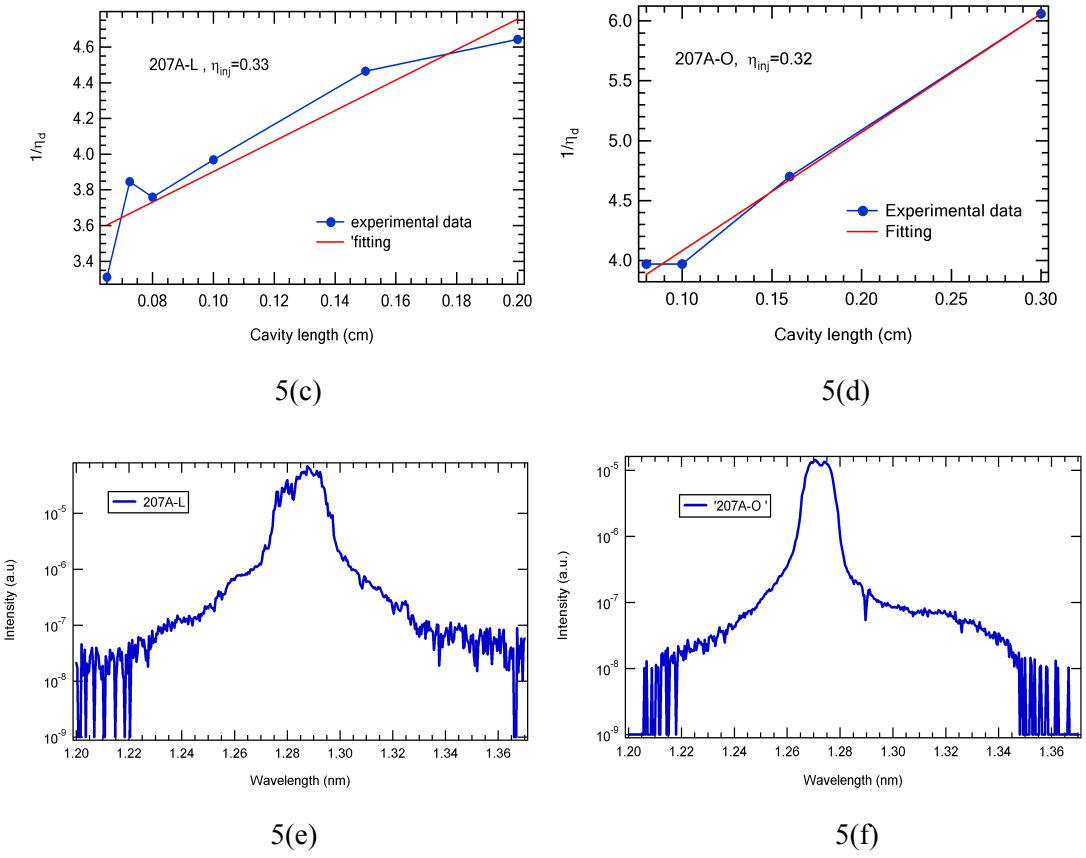

Figure 5. Laser performance data of 207A-L and 207A-O, maximum gain and transparency current (a) and (b), injection efficiency (c) and (d), and lasing spectra (e) and (f).

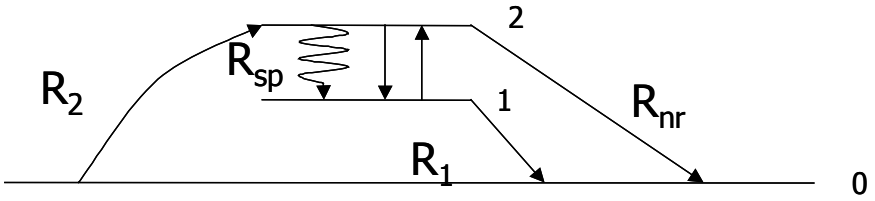

Figure 6. Schematic of the carrier recombination process in the quantum dot PL measurement.

4. β-PARAMETER MEASUREMENT

4.1 Theory

First, we introduce the β parameter to investigate the radiative and non-radiative recombination processes in the dots further. β is a parameter that describes the dominant process in the competition between radiative and non-radiative recombination rates. The total recombination rate in a semiconductor can be written as [7]

$$R_{rec} = R_{sp} + R_{nr} + R_{st} \qquad (1)$$

where R_{sp} is spontaneous recombination rate, R_{nr} is a non-radiative recombination rate, and R_{st} is the net stimulated recombination, including both stimulated absorption and emission. Using a three energy level approximation, a simplified model of the carrier recombination processes in the quantum dot material PL is plotted in figure 6. Pictured are the three energy levels labeled 0,1 and 2, a pumping rate R_2, the spontaneous (radiative) emission rate, R_{sp}, the non-radiative rate, R_{nr}, and a relaxation rate, R_1, from level 1 to 0. Stimulate emission occurs from level 2 to 1.

In the PL measurement, the stimulated emission process can be ignored. If $R_1 >> R_{sp}$, then $R_2 = R_{sp} + R_{nr}$ and for semiconductors, equation (1) can be written as

$$R_{rec} = AN + BN^2 + CN^3 \tag{2}$$

where N is the number of carriers. $R_{sp} = BN^2$ and R_{nr} is approximately equal to $AN+CN^3$. B is the bimolecular recombination coefficient. R_{nr} may be dominated by Shockley-Read-Hall (SRH) or Auger losses. For SRH, $R_{nr} = AN$. For Auger, $R_{nr} = CN^3$. In terms of measurable parameter, pumping power or current, eqn (2) can be changed to

$$\frac{P_{in}}{h\nu}\eta_{in} = AN + BN^2 + CN^3 \tag{3}$$

where P_{in} is the pumping power, η_{in} is a coupling coefficient to the illuminated sample. The output power (PL signal) can be expressed as

$$P_{out} = \eta_{out} h\nu R_{sp} \tag{4}$$

where η_{out} is output coupling coefficient to the collection optics. For different values of three recombination coefficients, A, B, and C, the recombination process may be dominated by one of three recombination rates listed above. If $A >> B$ and C, SRH is dominant, then

$$N = \frac{P_{in}}{Ah\nu}\eta_{in} \Rightarrow P_{out} \propto P_{in}^{\ 2} \tag{5a}$$

If $B >> A$ and C, then radiative recombination is dominant and

$$N^2 = \frac{P_{in}}{Bh\nu}\eta_{in} \Rightarrow P_{out} \propto P_{in} \tag{5b}$$

If $C >> A$ and B, Auger is dominant and

$$N^3 = \frac{P_{in}}{Ch\nu}\eta_{in} \Rightarrow P_{out} \propto P_{in}^{\ 2/3} \tag{5c}.$$

Therefore, in general, the relationship between the input pump power and the output power of the PL can be expressed as:

$$P_{out} \propto P_{in}^{\ \beta} \tag{6}$$

Clearly, the range of β is $2/3<\beta<2$. If $\beta > 1$, the dominant loss mechanism is SRH, if $\beta<1$, Auger is dominant.

4.2 Measurement results and discussion

The"M" and "H" piece from 207A were chosen to do the β parameter measurement due to their similarity to pieces "O" and "L", respectively. PL spectra under different pumping conditions are shown in Figures 6 (a) and (c). A 980 nm diode laser array was used as the pump source. The temperature was kept at 10°C during the measurement to minimize any heating effects. The output power was obtained by summing up all intensity data of the whole spectra. The relationship between the integrated PL intensity and the pump power (measured as the diode array bias current) is plotted in Figures 6(b) and (d) for "H" and "M" piece, respectively. The axes are set on a log scale so that the β can obtained by linear curve fitting. For piece"H", which was taken from the high PL intensity area, β is close to unity. That means the radiative recombination process is probably dominant given the relatively high PL intensity or, less likely, that the Auger and SRH processes balance out. For piece "M", which was taken from the low PL intensity area, β is 1.45. One can clearly state here that the SRH-related non-radiative recombination process is dominant. This result is consistent with our previous laser performance results and the transparency current density. "M" and "H" sample are next to "L" and "O", respectively, we can safely assume that β parameter is larger for sample "L". Thus, the high PL intensity and low transparency current in the "red" area (or upper right corner of the wafer) originates from smaller defect-related recombination rate and not increased dot density.

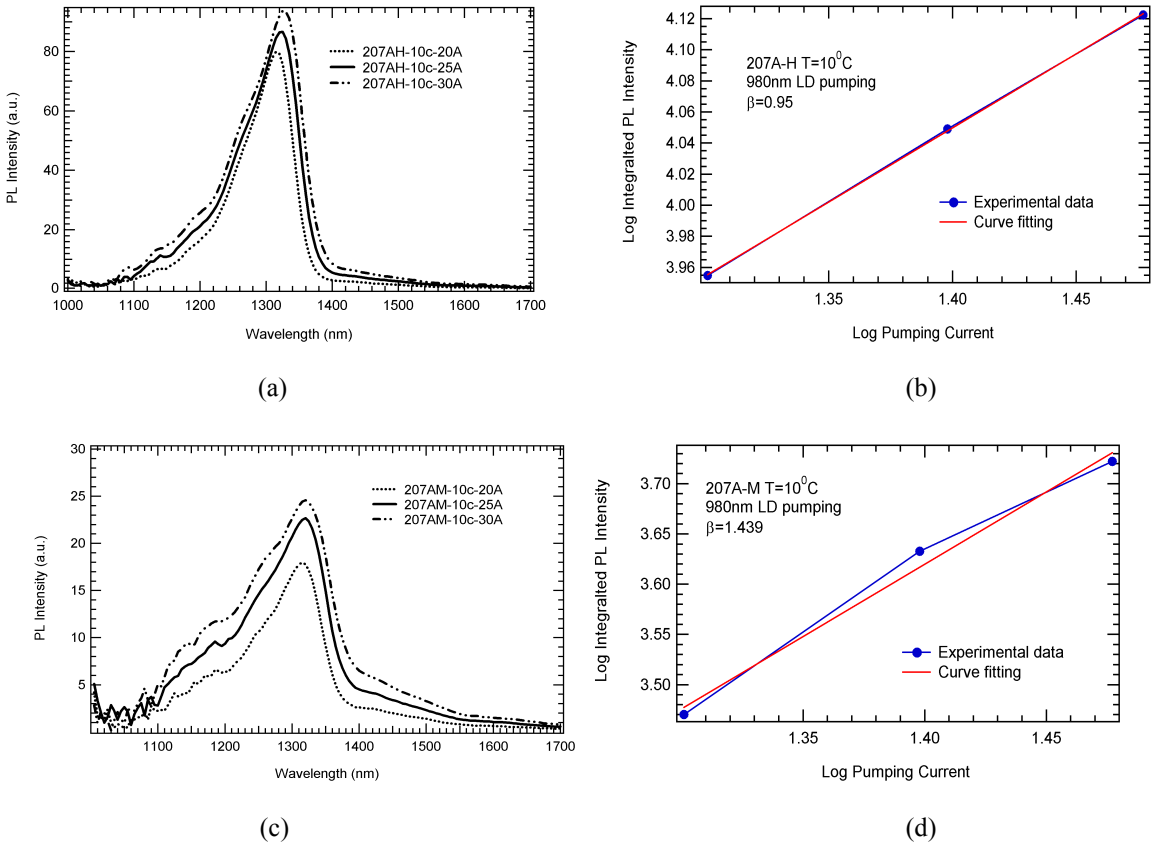

Figure 7. PL spectra under different pump power conditions (measured as the current supplied to the 980 nm laser diode array) for samples 207A-H, (a), and 207A-M (c), and the integrated PL intensity as a function of pump power for samples 207A-H, (b), and 207A-M, (d). The β parameter is calculated from the data in (b) and (d).

The β parameter may be different when we use a different wavelength pumping source because in the case of the 980 nm illumination, the GaAs barriers and waveguide around the DWELL structure is not excited. In Fig. 8, the variation of the integrated PL intensity with pump is shown using an 808 nm laser diode array that stimulates both the GaAs barriers and the active region. For the 808 nm case, the β of sample "M" is smaller than that of sample "H". Completely opposite to

the previous 980 nm pumping results. It may be interpreted as the effect of the GaAs barrier around the active region.. The defect density in GaAs layer may have a substantial effect on the overall output power and lead to a different β value overall.

5. CONCLUSIONS

Photoluminescence is an important tool to investigate optical properties of quantum dot material. In this study, by combining the PL spectrum measurement and laser performance data, we conclude that variations in PL intensity from within a wafer originate primarily from differences in the defect recombination rates and not from dot density variation. There are some questions still remaining for further discussion. First one is how to determine where the defect recombination is actually occurring. In the GaAs barrier, the QW around the dots, or the dots themselves? Different PL behavior with a different pumping wavelength shows some clues but still need further verification. If the defects are in the dots, how big is the effect? Will the dots remain non-radiative for all pump values (dark dots), or can be they activated under high external pumping? Is it possible to identify the density of completely non-radiative dots? This may be the most challenging problem here.

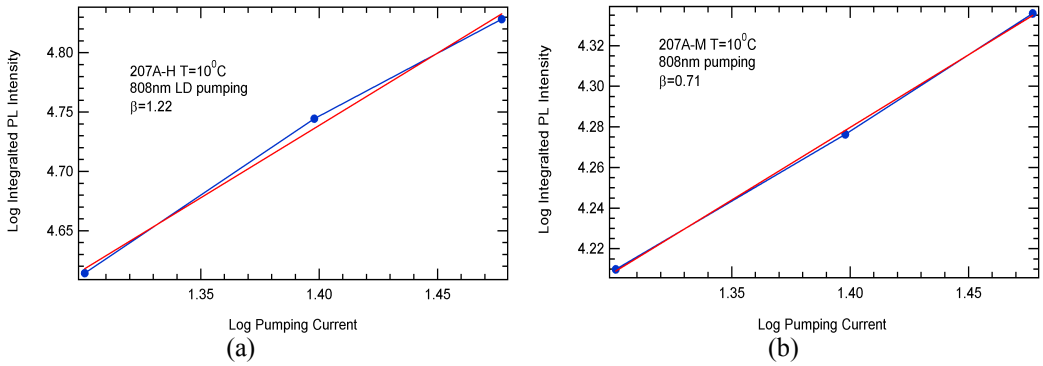

Figure 8. β parameter of 207A-M and 207A-H samples, measured using an 808 nm laser diode pump array.

REFERENCES

1. D. Bimberg, N. Kirstaedter, N. N. Ledentsov, Zh. I. Alferov, P. S. Kopíev, and V. M. Ustinov, *InGaAs-GaAs Quantum-Dot Lasers*, IEEE J. of Select. Top. Quantum Electron, vol. 3, pp. 196-205, 1997.
2. L. F. Lester, A. Stintz, H. Li, T. C. Newell, E. A. Pease, B. A. Fuchs, and K. J. Malloy, *Optical Characteristics of 1.24 μm InAs Quantum-Dot Laser Diodes*, IEEE Photon. Technol. Lett., vol .11, pp. 931-933, 1999.
3. G. T. Liu, A. Stintz, H. Li, T. C. Newell, A. L. Gray, P. M. Varangis, K. J. Malloy, and L. F. Lester, *The Influence of Quantum-Well Composition on the Performance of Quantum Dot Lasers Using InAs/InGaAs Dots-in-a-Well (DWELL) Structures*, IEEE J. of Quantum Electron, vol. 36, pp. 1272-1279, 2000.
4. H. Chen, Z. Zou, O. B. Shchekin, and D.G. Deppe, *InAs quantum-dot lasers operating near 1.3μm with high characteristic temperature for continuous-wave operation*, Electron. Lett, vol. 36, pp. 1703-1704, 2000.
5. T. C. Newell, D. J. Bossert, A. Stintz, B. Fuchs, K. J. Malloy, and L. F. Lester, *Gain and Linewidth Enhancement Factor in InAs Quantum-Dot Laser Diodes*, IEEE Photon. Technol. Lett., vol .11, pp. 1527-1529, 1999.
6. A. Stintz, G. T. Liu, A. L. Gray, R. Spillers, S. M. Delgado, and K. J. Malloy, *Characterization of InAs quantum dots in strained $In_xGa_{1-x}As$ quantum wells*, J. Vac. Sci & Technol. B18, 1496-1501, 2000.
7. L. A. Coldren, S. W. Corzine, *Diode Lasers and Photonic Integrated Circuit*, Wiley ,New York ,1995.